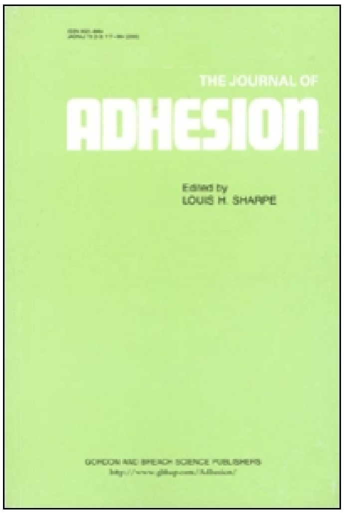

The Journal of Adhesion
Publication details, including instructions for authors and subscription information:
http://www.informaworld.com/smpp/title~content=t713453635

Analysis of Contact and Rupture Behaviour Under Non-Constant Contact Surface Conditions

J. F. Ganghoffer[a]; J. Schultz[a]
[a] ICSI, Mulhouse Cedex, France

To cite this Article Ganghoffer, J. F. and Schultz, J.(1998) 'Analysis of Contact and Rupture Behaviour Under Non-Constant Contact Surface Conditions', The Journal of Adhesion, 65: 1, 25 — 56
To link to this Article: DOI: 10.1080/00218469808012237
URL: http://dx.doi.org/10.1080/00218469808012237

J. Adhesion, 1998, Vol. 65, pp. 25–56
Reprints available directly from the publisher
Photocopying permitted by license only

Analysis of Contact and Rupture Behaviour Under Non-Constant Contact Surface Conditions

J. F. GANGHOFFER* and J. SCHULTZ

ICSI, 15, Rue J. Starcky, BP 2478, 68057 Mulhouse Cedex, France

(Received 26 July 1995; In final form 8 January 1997)

The present paper addresses the problem of contact between a rigid hemisphere and a thin elastic layer strongly bonded on a rigid plane support, which can be thought of as an adhesive obeying a geometrically non-linear behaviour due to the change of contact area. Using the asymptotic expansion method from a three-dimensional analysis of the layer, a two-dimensional model is derived, under the assumptions of large displacements and small strains. The leading term of the solution of the asymptotic development is such that the displacement field varies linearly through the layer thickness and the stress tensor is constant. A quasi-linear relation is obtained between the area of contact and the penetration of the hemisphere within the layer, and the variation with penetration of the compressive load exerted by the hemisphere is seen to give satisfactory agreement with experiments. In the last part, we present theoretical results concerning the rupture behaviour; the effect of adhesion energy between the hemisphere and the layer on the radius of curvature at the rupture point between both solids is assessed. Further, the thickness of an hypothetical interphase through which failure propagates is determined theoretically.

Keywords: Contact problems; non flat surfaces; thin layers; curvature effects; adhesion; perturbation methods

1. INTRODUCTION

The derivation of simplified mechanical models of thin films is usually done by making assumptions concerning both the kinematics of the film and relative order of magnitude of strains and stresses. A pioneering work by Goland and Reissner [1] can be considered as a first

*Corresponding author.

attempt towards a structural constituent describing an elastic adhesive. From that, both closed form solutions and special finite elements were developed, in which the mechanical fields do not depend on the thickness co-ordinate, *i.e.* the adhesive can be considered as a material surface. Simplified theories for a wide range of structural constituents such as plates, beams, shells have been obtained by this way, where the two-dimensional model still displays significant original features of the original three-dimensional problem.

Alternatively, the derivation of a simplified theory for structural constituents can be done using the asymptotic method, through which the classical simplified models are recovered in a deductive way, *i.e.* without any *a priori* assumptions due to the thinness of the film, see Mitropoulos [2], Klarbring [3] or Ciarlet [4].

In asymptotic methods, one tries to construct the solution of the three-dimensional problem as a series development of the unknowns in terms of a small non-dimensional parameter ε (for instance, the ratio of the plate thickness to a characteristic macroscopic length); the first term in the series represents the limit as $\varepsilon \rightarrow 0$, which is an approximation of the original problem (Ciarlet *et al.* [4] and Verhulst [5]). Asymptotic analysis relies methematically (and particularly considering the open problem of convergence of the asymptotic development for a finite value of ε) on the general techniques developed by Lions [6] for handling linear variational problems containing a small parameter. Methods of asymptotic expansion has been shown to provide a powerful and systematic (although rather formal) tool for justifying two-dimensional plate theories, in both the linear and non-linear cases: the leading term of the asymptotic development of the three-dimensional solution indeed solves the classical equations of the plate theories, with fewer assumptions and, therefore, greater understanding and confidence. Compared with traditional plate theory, the asymptotic method provides more information about the general three-dimensional solution, since it gives additional higher order terms and boundary layer terms.

Asymptotic methods were first applied to plate problems posed as partial differential equations: in that case, some *a priori* assumptions are still needed. For instance, Goldenveizer [7] assumes that the effect of volumic forces can be neglected and that the required state of strain and stress is skew-symmetrical about the middle-plane. In addition, some difficulties arise concerning the kind of boundary conditions to be considered for the successive terms of the asymptotic expansion (Friedrichs *et al.* [8]). A further source of difficulty lies in the absence of a satisfactory convergence analysis, due to both the setting-up of the problem as a set of differential equations (instead of a single one) and the lack of a maximum principle (Eckhaus [9]).

More recently, Ciarlet *et al.* [4] applied asymptotics to three-dimensional linear plate problems posed in a mixed variational form (displacement-stress approach) called the Hellinger-Reissner variational principle (Washizu [10] and Valid [11]). In that approach, both the displacement and the stresses are considered as unknowns, and such a setting has been shown by previous authors to be the natural one for proving convergence of the development, and for obtaining error estimates.

Quite recently, Klarbring [12] developed an asymptotic model of elastic adhesively bonded joints on the same basis; the author assumed that the modulus of the adhesive scales as $E = \varepsilon \cdot E_0$, where E_0 has the order of magnitude of the adherend modulus. The first order solution is then such that the displacement field varies linearly through the plate thickness, whereas the Cauchy stress field is constant.

Consideration of the geometrically non-linear behaviour of certain types of adhesives implies that a numerical analysis is necessary in most cases. These effects were already taken into account in the work by Goland and Reissner [1] by imposing secondary loads. Considering more recent works, Reddy and Roy [13] derived a finite element for an adhesive in a two-dimensional elastic plane stress small strain situation, using an updated Lagrangian approach. More complicated constitutive behaviour of the adhesive was considered in parallel works by the same author, including non-linear visco-elasticity and effects of diffusion of moisture.

Klarbring [14] derived a simplified description of an elastic adhesive layer connecting two stiff bodies, in which the displacement is assumed to vary linearly through the thickness of the adhesive. A virtual work equation is derived using a total Lagrangian formulation, and the equations are linearized, which enables a finite element treatment using Newton method. This modelling has been applied to the single lap joint and the cantilever beam.

An extensive study of adherence between rigid cylindrical bodies and elastic or viscoelastic materials (elastomers) has been done by

Maugis and Barquins [15, 16]; in these works however, the case of a thin elastic layer is not envisaged. Non-conformal contact problems such as the one treated here can not be calculated solely using Hertz theory, since one must consider the shape of the bodies and the way they are supported; an extensive analysis of contact problems involving cylindrical bodies can be found in the book by Johnson [17], and in the many references therein. A paper by Matthewson [18] gives an analytical solution for the indentation of a thin soft elastic coating by a rigid indenter, using Bessel's functions. Considering the indentation by a rigid hemisphere, the author obtains an excellent agreement between the theory and experimental measurements of both contact radius and penetration *versus* the applied load.

In the present work, we first use the asymptotic method in order to derive a two-dimensional simplified model of a thin plate undergoing large displacement, which is a generalisation of the asymptotic analysis of the same problem in a small displacement situation Klarbring [12].

2. SOLUTION OF THE CONTACT PROBLEM BETWEEN A RIGID HEMISPHERE AND A THIN ELASTIC LAYER

2.1. Relation between Area of Contact and Penetration

A rigid hemisphere (radius R) is brought into frictionless contact with a thin elastic layer (thickness t, modulus E, Poisson's ratio ν), being glued on a rigid plane support; a diagrammatic view of the system is presented on Figure 1.

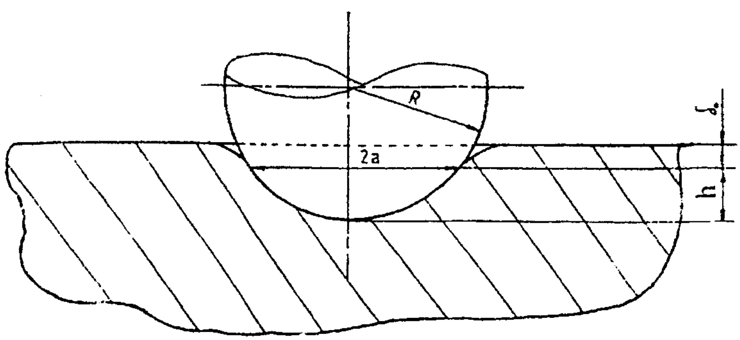

FIGURE 1 Contact between a rigid hemisphere and a soft elastic layer.

Due to the fact that the contact occurs on a varying surface, when the penetration of the hemisphere increases, there is a geometrical non-linearity. As a prerequisite to the solution of this problem, we then first establish the contact law for a thin elastic film undergoing geometrical non-linear effects.

The generic problem considered is then the following: we consider two bodies Ω_1^ε and Ω_2^ε joined (adhesively or not) by a thin elastic layer Ω_0^ε of thickness 2ε, considered small compared with the dimensions of Ω_1^ε, Ω_2^ε. The two bodies Ω_1^ε and Ω_2^ε will be called adherends in the following, while the thin body Ω_0^ε is termed adhesive. $\Omega_0^\varepsilon = \omega \times (-\varepsilon, \varepsilon)$ is supposed to be a cylindrical body with boundary $S_0^\varepsilon = \gamma \times [-\varepsilon, \varepsilon]$; the two contact surfaces between the adhesive and the adherends are $S_1^\varepsilon = \omega \times (\varepsilon)$ and $S_2^\varepsilon = \omega \times (-\varepsilon)$, Figure 2.

The placement of the three bodies is a continuous mapping

$$\phi : \bar{\Omega}^\varepsilon \to R^3,$$

where $\Omega^\varepsilon = \Omega_1^\varepsilon \cup \Omega_2^\varepsilon \cup \Omega_0^\varepsilon$ and $\bar{\Omega}^\varepsilon$ denotes its closure. The displacement is then a mapping

$$u : \bar{\Omega}^\varepsilon \to R^3$$

$$\phi = \mathrm{Id} + u, \tag{1}$$

where Id is the identity map. The Green strain tensor is then defined according to

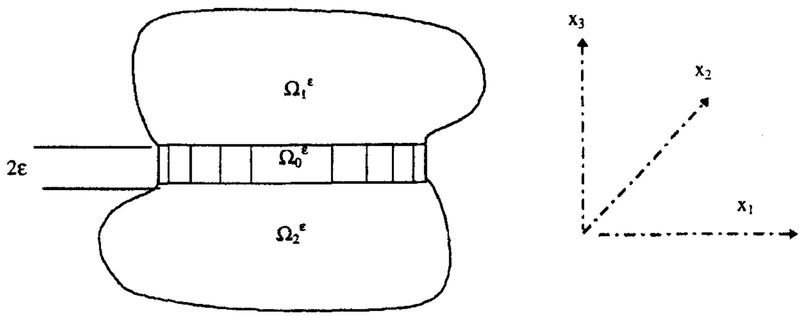

FIGURE 2 Geometry of the three-dimensional adhesive joint problem.

$$E(\phi) = \frac{1}{2} \cdot \left(\frac{\partial \phi}{\partial X_i} \cdot \frac{\partial \phi}{\partial X_j} - \delta_{ij} \right) \cdot E_i \otimes E_j \tag{2}$$

where the standard basis $(E_i)_i$ of R^3 is used.

All three bodies are considered linear elastic, the adherends having a possible anisotropic behaviour expressed by the constitutive relation $\sigma_{ij} = A_{ijkl} e_{kl}$, where e is the small strain tensor, the linear part of E; the previous relation can be inverted, so that $e_{ij} = a_{ijkl} \cdot S_{kl}$. This means that we assume that the adherends experience only small strains. In the following, Latin indices take their values in the set $\{1, 2, 3\}$, while Greek indices take their value in the set $\{1, 2\}$.

As a matter of simplicity, the adhesive is assumed to be isotropic with tensile modulus E and Poisson's ratio ν, so that it satisfies the S^t Venant-Kirchhoff constitutive law

$$E_{ij} = \frac{1+\nu}{E} S_{ij} - \frac{\nu}{E} \delta_{ij} S_{kk}, \tag{3}$$

where S is the symmetric second Piola-Kirchhoff stress tensor.

E and ν are allowed to be functions of the two first coordinates, but not of the third. Body forces $\underline{f}$ are applied to all bodies, and surface tractions $\underline{t}$ are applied to the parts S^{ε}_{1t}, S^{ε}_{2t} of the boundaries $\partial\Omega^{\varepsilon}_1$, $\partial\Omega^{\varepsilon}_2$ respectively, whereas the lateral surface of Ω^{ε}_0 is supposed to be free of effort. The adherends are held fixed; $\underline{u} = 0$ on the parts S^{ε}_{1u}, S^{ε}_{2u} of $\partial\Omega^{\varepsilon}_1$, $\partial\Omega^{\varepsilon}_2$, respectively.

The derivation of the contact law between the hemisphere and the thin layer is presented in Appendix 1, using an asymptotic method. The placement is found to vary linearly through the adhesive thickness (therefore also the displacement, as found also by Johnson [17] in his treatment of contact mechanics), so that the normal components of the strain tensor are given by

$$E_{33} = w_3 = \frac{1}{2}\left(\frac{\Delta\phi \cdot \Delta\phi}{h^2} - 1 \right), \quad \text{with } \Delta\phi = (\phi^1 - \phi^2) \tag{4}$$

$$E_{3\alpha} = \frac{1}{2} w_\alpha = \frac{1}{2}\left(\frac{\Delta\phi}{h} \cdot \frac{\partial \phi_0}{\partial X_\alpha} \right), \quad \text{with } \phi_0 = \frac{1}{2}(\phi^1 + \phi^2) \tag{5}$$

The strain tensor solution of the first order problem is then completely characterised by equalities (A11a), (4) and (5).

The same strain measures have been obtained by Klarbring [12]; asymptotic analysis however enables one to deduce the same simplified model of the adhesive with an increased accuracy, according to additional relations (A9a, b, c, d, e), (A10a, c, d, e) and (A11a, b), see Appendix 1. The novelty of this contribution is, thus, the establishment of a simplified model of an adhesive undergoing large displacements in a deductive manner.

We are now in a position to derive a contact law for a thin elastic film undergoing geometrically non-linear effects. The generalised strain measures are defined by Equations (15), (16), and the associated stress measures by

$$p_i = \int_{-h/2}^{h/2} S_{3i} \cdot dz \tag{6}$$

The constitutive Equation (3) implies that the p_i are related to the w_i through

$$p_i = C_{ij} w_j, \tag{7}$$

with

$$(C_{ij}) = \frac{Et}{(1+\nu)} \begin{pmatrix} 1/2 & 0 & 0 \\ 0 & 1/2 & 0 \\ 0 & 0 & \dfrac{1-\nu}{1-2\nu} \end{pmatrix} \tag{8}$$

For a given total penetration, V, of the hemisphere into the elastic layer, contact of the layer onto the surface of the hemisphere occurs at the height h, while the remaining part δ_0 is the penetration of the edge of the contact zone relative to the free surface at infinity. Therefore, one has

$$V = h + \delta_0 \tag{9}$$

Considering volumic forces, f, and tractions, g, applied on the boundary, the principle of virtual work expresses as

$$\int_{\Omega} S : \delta E(\phi, \delta\phi) \cdot dV = \int_{\Omega} f \cdot \delta\phi \cdot dV + \int_{\partial\Omega} g \cdot \delta\phi \cdot dS, \tag{10}$$

which should hold for any admissible variation $\delta\phi$.

We assume now that volumic forces are negligible and that both the hemisphere and the support on which the elastic layer is glued are rigid, so that their contribution to (10) is null. Further, the boundary conditions are those of imposed traction on the upper surface of the hemisphere, and null efforts on the remaining surface of the elastic layer; since the contact between the elastic layer and the hemisphere is assumed perfect (no relative displacement occurs), and since the hemisphere is rigid, it is seen that the virtual work of applied tractions expresses as $\int_{S_c} g_3\, \delta\phi_3\, dS$, where Sc is the contact area. In the limit of a layer having a vanishing thickness, this integral becomes $\int_{\omega} p_3 \cdot \delta w_3 \cdot d\omega$.

Measures of strains and stresses for a thin film derived in the previous section imply that the virtual work of the stresses done within the layer expresses as

$$\delta W^{(L)} = \int_{\omega} p_i \cdot \delta w_i \cdot d\omega = \int_{\omega} p_3 \cdot \delta w_3 \cdot d\omega, \tag{11}$$

according to (10) and to the previously derived expression of the virtual work of the tractions. The generalised strain measures are defined by Equations (4), (5), and the associated stress measures by (6). The area of contact, A, between the hemisphere and the layer is related to the height, h, through

$$A = 2 \cdot \pi R h = \pi \cdot (a^2 + h^2), \tag{12}$$

We now derive the integral over the contact area in (10) with respect to the radius a, which gives

$$C_{rr} \cdot w_r(a) \cdot \delta w_r(a) + C_{zz} \cdot w_z(a) \cdot \delta w_z(a) = C_{zz} \cdot w_z(a) \cdot \delta w_z(a), \tag{13}$$

resulting in

$$C_{rr} \cdot w_r(a) \cdot \delta w_r(a) = 0, \quad \forall\, \delta w_r(a) \tag{14}$$

We consider the kinematics of points lying on the upper surface of the layer: points already in contact with the hemisphere remain in contact, so that their displacement is purely normal. We suppose that points entering into contact experience mainly a normal displacement, and so we neglect in the following the radial component of the displacement. Therefore, one has

$$w_r(a) = \frac{V}{t} + \frac{\partial u(a)}{\partial r}\left(\frac{V}{2t} + \frac{1}{2}\right), \tag{15}$$

where $u(a)$ is the normal displacement of the material point that coincides with the geometrical contact point.

Equation (25) implies, then, following differential equation

$$\frac{V}{t} + \frac{\partial u(a)}{\partial r}\left(\frac{V}{2t} + \frac{1}{2}\right) = 0 \tag{16}$$

The gradient of the displacement at the edge of the contact zone is then

$$g = -\frac{2V}{V+t} \tag{17}$$

According to this, the displacement of a point lying initially on the free surface of the layer that comes into contact with the hemisphere is $u(a + \Delta a) = u(a) + \Delta u = u(a) + g \cdot \Delta a$, so that the derivative $du(a)/da$ is

$$\frac{du(a)}{da} = -\frac{2V}{V+t} \tag{18}$$

Using the relations $u(a) = V - h$; $da/dA \approx 1/2(\pi A)^{1/2}$, the penetration, V, solves the following differential equation:

$$\sqrt{A}\frac{dV}{dA} + \left(\frac{V}{V+t}\right)\frac{1}{\sqrt{\pi}} = \frac{\sqrt{A}}{2\pi R} \tag{19}$$

We consider the behaviour of the film under small compressions, so that the displacement, V, is negligible with respect to the thickness (V/t is less than 0.1); Equation (19) then simplifies to

$$\sqrt{A}\frac{dV}{dA}+\frac{V}{t}\frac{1}{\sqrt{\pi}}=\frac{\sqrt{A}}{2\pi R} \tag{20}$$

The integration is easy, so that the penetration is related to the contact area through

$$V(A)=\frac{t^2}{4R}\cdot\left(\left(\frac{2\cdot\sqrt{A}}{t\cdot\sqrt{\pi}}-1\right)+\exp\left(-\frac{2\cdot\sqrt{A}}{t\cdot\sqrt{\pi}}\right)\right), \tag{21}$$

and it can be checked that the area of contact is related to the penetration, V, through $A=2\pi RV$ when V tends to zero, which means that the height of the edge of the contact zone is null.

We note from Equation (19) that the relation between contact area and penetration does not depend on the mechanical properties of the layer, whereas the approximate solution (21) shows that the area of contact can be related to the penetration through $A=\pi R\cdot f(V, k(t))$, where the parameter $k(t)$ depends only on the thickness of the layer.

We further examine the consequence of relation (21) when the penetration is still small, but finite: the exponential term can be described by its linear development, when the variable $2\sqrt{A}/t\sqrt{\pi}$ is less than 0.1, which implies a ratio V/t less than 2×10^{-4}. One then has the following linear relation between the penetration, V, and the area of contact,

$$A=k(t)\pi RV.$$

In that case, we represent the area of contact *versus* penetration in a practical situation where $R=20$ mm and $t=3.29$ mm, with which the theory will be compared in Section 3.

Figure 3 shows that the area of contact varies nearly linearly with the penetration, so that $A=1.6\pi RV$, considering values of the ratio V/t less than 5×10^{-4}. It is seen, therefore, that deviations from the limiting behaviour ($A=2\pi RV$) already occur for very small penetrations.

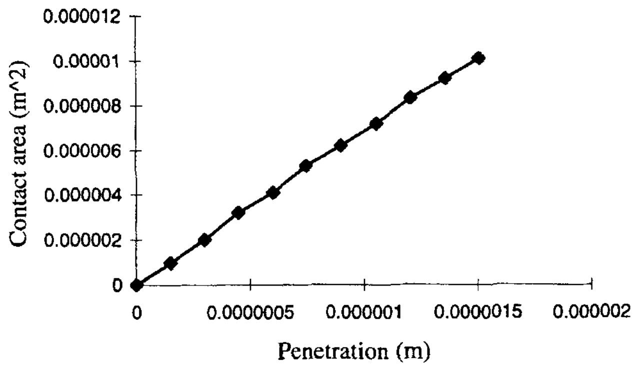

FIGURE 3 Relation between contact area and penetration (Equation (21)).

2.2. Relation between Compressive Effort and Penetration

The force exerted by the hemisphere on the elastic layer is the integral over the contact area

$$F = \int_{\omega} S_{zz} d\omega , \tag{22}$$

where

$$S_{zz} = \frac{E(1-\nu)}{(1+\nu)(1-2\nu)} E_{zz} = K^u w_3 , \tag{23}$$

where K^u is the uniaxial compressibility modulus of a layer having modulus E and Poisson's ratio $\nu (K^u = E(1-\nu)/((1+\nu)(1-2\nu)))$, so that the derivative of the force *versus* the displacement, V, is given by

$$\frac{dF}{dV} = \frac{dF}{dA}\frac{dA}{dV} = k(t)\pi R K^u w_3 , \tag{24}$$

where the strain w_3 is evaluated from Equation (15):

$$w_3 = \frac{V}{t} + \frac{1}{2}\left(\frac{V}{t}\right)^2 \approx \frac{V}{t}, \tag{25}$$

for small penetrations. Relation (25) is then easily integrated, and the force-displacement relation is

$$F(V)=\frac{k(t)\,\pi RK^{u}}{2t}\,V^{2}. \tag{26}$$

3. COMPARISON WITH EXPERIMENTAL MEASUREMENTS

A glassy transparent hemisphere (radius 20 mm) is brought into contact with a thin SBR layer (a commercial elastomer with 0.5% DCP, with a thickness of 3.29 mm) being strongly adhered to a rigid plane support; the apparatus used for measurements of contact area is sketched below (Fig. 4). The area of contact is illuminated by reflection of monochromatic light, and is observed through the transparent hemisphere with a binocular microscope. The hemisphere is supported by a balance, which is moved vertically at a constant speed (a low velocity of 0.2 mm/min and a high velocity of 20 mm/min were used) *via* a computer-controlled transducer; the displacement is recorded with a precision of about 1 μm. Different magnifications can be used and both intensity and orientation of the light source could be adjusted, so that the radius of contact could be obtained with a precision

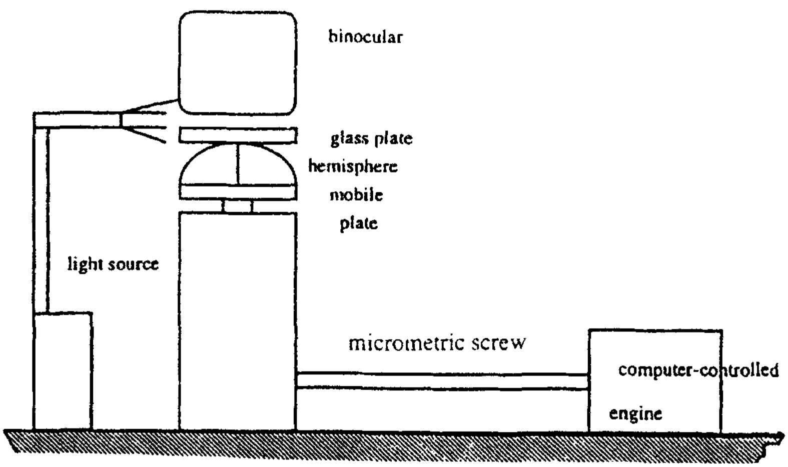

FIGURE 4 Apparatus for measuring the area of contact.

of about 10 μm. Note, however, that the edge of the contact area presents irregularities for small penetrations (less than 0.03 mm), so that the precision of measurement is decreased. In order to remedy that, chains of silane are grafted on the surface of the glassy hemisphere (when the chains are long enough, they interdiffuse within the elastomer), in order to get a nearly perfect adhesion condition at the interface. The coupling agents used were organo-silanes, one extremity of which reacts with the glass surface, whereas the other extremity is compatible with the polymeric material. The area of contact was measured both during compression and subsequent unloading. Only the projection of the true area of contact on a horizontal plane could be measured. For a radius of the plane contact area, a, the three-dimensional area of contact, A (it is a portion of the hemisphere surface), is then reconstructed from Equations (10) and (12). When making the optical measurements, care must be taken, because the error in determining the contact edge can be large when the contact diameter is small, so that a correction for optical effects is in fact required: the accuracy of radius measurement on the binocular microscope is thus reduced to the order of 0.1 mm.

In all situations, the measured area is found to vary linearly with the total penetration; the slope of the relation $A(V)$ is compared (Tab. I) with the value corresponding to the situation in which the edge of the contact zone has the same height as the free surface of the layer (slope equal to 79.6).

The slope is nearly the same whatever the velocity and loading condition, and the area of contact is found to vary linearly with the total penetration according to:

$$A \cong \frac{3}{2}\pi \cdot R \cdot V, \tag{27}$$

TABLE I Measurement of the contact area *vs.* penetration depth

Load situation	compression	compression	traction	traction
Velocity (mm/min)	0.2	20	0.2	20
Experimental slope dA/dh (mm^2/min)	60.8	63.4	59	60.2
Relative variation (%)	20.4	23.6	24.3	25.8

and we note that the slope in this relation does not depend on the material properties of the contacting solids (it is only a function of their geometry). The height, h, of the portion of sphere on which true contact occurs is then easily deduced to be:

$$h \cong \frac{3}{4} V, \tag{28}$$

so that the height of the edge of the contact zone still represents one quarter of the total penetration:

$$\delta_0 \cong \frac{V}{4}. \tag{29}$$

Comparison of the experimental measurement of contact area Equation (27)), with the theoretical relation obtained in Section 3.1 ($A = 1.6\pi RV$) shows that the theory correctly describes the experimental result: the coefficient $k(t)$ is 1.5 according to the theory (Equation (27)), whereas the measured value is 1.6. Measurements of the forces necessary to compress the hemisphere onto the elastic were performed on a traction machine. The hemisphere (made of steel, radius 20 mm) is moved at a constant velocity (1 mm/min), and cylindrical sheets of elastic materials of different thickness (0.37 mm; 1.39 mm; 1.84 mm; 3.29 mm; 9.8 mm; 19.6 mm) were glued on a rigid baseplate. The diameter of the elastic sheets was chosen large enough so that it could be considered as infinite compared with the radius of the contact area. The experimental relation between force and penetration is shown in Figure 5 using logarithmic scales for both axes. The variable represented on the vertical axis is the force multiplied by the thickness of the layer, so that the effect of the thickness is described.

A linear relation is obtained, with a relatively large scatter: the slope lies in the interval 1.29–1.75. The shape of the curves implies that the force/penetration function takes the power law form:

$$F = \frac{C}{t} V^{\alpha}, \tag{30}$$

where C and α are constants. The values of the exponent, α, obtained for the different thicknesses present a relatively large scatter around a

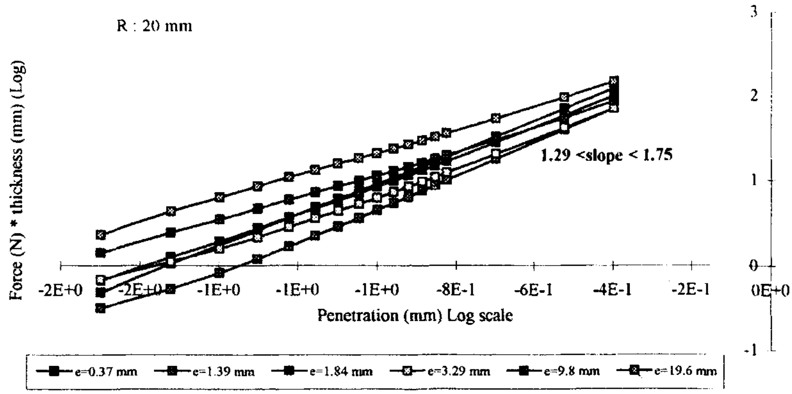

FIGURE 5 Compressive effort *vs* penetration exerted by a rigid hemisphere on a thin elastic layer.

central value equal to about 1.5. Note that since the force exerted by the hemisphere on the elastic sheet is inversely proportional to its thickness, it is seen that an infinite force would be needed to compress a sheet of vanishing thickness.

Comparison of this relation with the experimental curve for a 3.29 mm thick layer being compressed by a hemisphere having 20 mm radius (the modulus of the layer has been measured as about 1 MPa, and the contraction coefficient is taken as 0.49 to represent a nearly incompressible rubbery material) shows that (Fig. 6) the analytical solution (Equation (26)) slightly underestimates the measured force, with a nearly constant shift over the whole range of penetrations. In the present case, the coefficient in front of V in Equation (30) takes the value 1.68×10^8. The relation between load and penetration given by Hertz theory is $F = KR^{1/2}V^{3/2}$, with $K = 4E/3(1 - \nu)$. Considering the same values of the parameters, the coefficient $KR^{1/2}$ takes then the value 3.7×10^5, so that it can be seen that Hertz theory gives a correct agreement with the present model (Tab. II).

Compression experiments performed on the same material but with a rigid flat punch (the contact area is then constant) have evidenced that the global response of the layer over the range of penetrations shown on Figure 6 is still linear, so that a possible hyperelastic material behaviour can not be considered as responsible for the observed discrepancy. On the other hand, it is seen that a small departure from

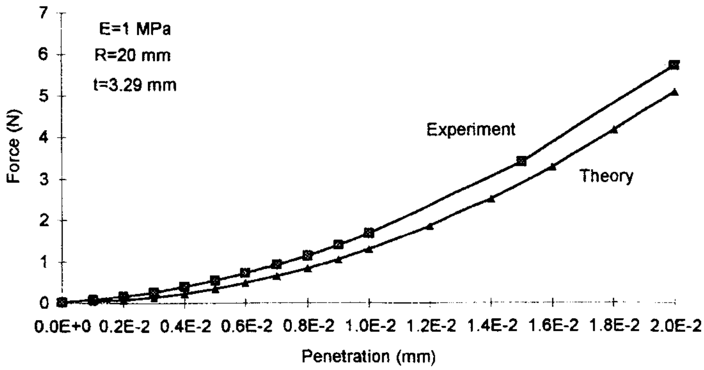

FIGURE 6 Comparison between experimental and theoretical force-displacement relation.

TABLE II Relationship between force and penetration. Comparison between Hertz model and the present theory

Penetration (mm)	0.001	0.01	0.1
Force (N) Hertz model	3.7×10^{-4}	1.17×10^{-2}	0.37
Force (N) present model	1.68×10^{-4}	1.68×10^{-2}	1.68

complete incompressibility will cause a strong change in the compressibility modulus in Equation (26) and, therefore, in the compression effort. This points towards the need for accurate measurements of Poisson's ratio; not withstanding this, a relatively good agreement is obtained (particularly, the proportionality of the force with the inverse of the thickness is satisfied).

4. THEORETICAL STUDY OF THE RUPTURE BEHAVIOUR

We try to describe the curvature effects at the edge of the contact zone, with considerations of adhesion effects; analytical models in the literature describing the penetration of an infinite half-space by a rigid hemisphere all lead to a constant curvature-independent of the penetration:

–the solution by Sneddon [19] gives a radius of curvature equal to the radius of the hemisphere

–Maugis and Barquins [18] established a model in which adhesion effects could be considered. In both cases (with and without adhesion), it is found that the elastic block leaves the surface of the hemisphere with an infinite curvature.

In these models, the essential difficulty lies in an accurate evaluation of the displacement field of the surface of the elastic film under compression, which forms the starting point of the analysis. We now propose a different approach, not being based on the mere knowledge of the displacement field. A magnification of the edge of the contact zone along the tangent plane is performed, which evidences an "interior" zone where the film is in contact with the hemisphere, and an "exterior" zone where the film leaves the surface of the hemisphere (there is no more contact); the distribution of stresses will then be described by the asymptotic solution for weakly curved shells.

4.1. Thickness of the Interphase between the Hemisphere and the Elastic Layer

The unloading of the hemisphere from the film can be described as the propagation of a crack at the interface between both materials, and it is assumed that physical links are broken within a thin region (the interphase) of constant thickness, t. The term interphase denotes the boundary polymeric layer developed between successive phases in composites; this transition region is characterised by a molecular structure different from that of the bulk neighbouring phases. The nature, extent and properties of the interphase depend in an essential way on the kind of material on either side. The transition layer between two polymers is characterised by mixed molecular structure and diffusion phenomena, such as the interpenetration of the segments of the polymer chains; in this fact lies the essential difference of the interphase formed by two polymers and the layer formed by a polymer and an inorganic solid (Theocaris [20]). Considering the last situation, Theocaris proposed a theoretical model for fibrous composite materials for both determination of the thickness and law of variation of the mechanical properties of the interphase developed between an inert fiber and a polymeric matrix. In this so-called unfolding model, the mechanical properties of the interphase are assumed to change continuously from that of the fiber to the matrix properties; a good agreement was found for the extent of the interphase determined theoretically and experimentally by calorimetric measurements of the jump in the heat capacity of the polymeric composite as its glass transition temperature.

The rupture stress at the point of contact, σ_R, is determined considering that the film can be locally identified with a thin plate (this is justified by the fact that curvature effects on the contact zone are small, since the radius of the hemisphere is large), so that $\sigma_R = \sqrt{2 \cdot Ku \cdot Ga}/\sqrt{t}$, Destuynder [21], where Ga is the interfacial adhesion energy and K_u the uniaxial compressibility modulus of the layer. In a Cartesian co-ordinate system, the vertical contribution of this stress is $\sigma_R \cdot \cos^2\theta_c$, which represents, in fact, the derivative of the rupture force with respect to the area of contact. One has further that $\cos\theta_c = 1 - h/R$, so that the rupture force has the following dependence on the contact area:

$$F^R(A) = \frac{\sqrt{2 \cdot Ku \cdot Ga}}{\sqrt{t}}\left(A - \frac{A^2}{2\pi R^2} + \frac{A^3}{12\pi^2 R^4}\right). \qquad (31)$$

The thickness of the interphase is then determined by the identification of the slope $dF^R(A)/dA$ for small compressions in Equation (31) with the experimental value (Fig. 7).

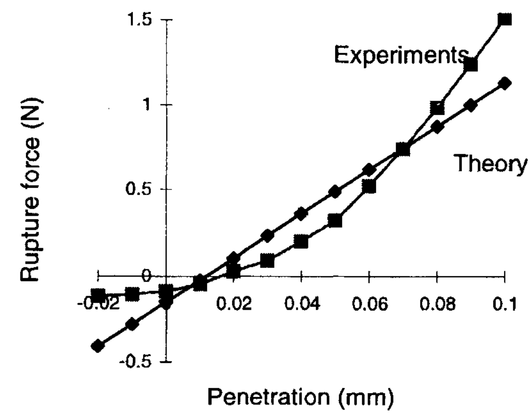

FIGURE 7 Rupture force *vs.* penetration.

Adhesion energy for the film of thickness 3.29 mm has been measured (by peeling) as 365 J/M^2, so that the interphase thickness is identified as 0.75 microns. As a matter of comparison, application of the Theocaris model to a fibrous composite made of glass fibers (radius of the fibers is about 63 microns) embedded in a epoxy resin matrix results in an interphase thickness of about 1 micron (Theocaris [20]); the thickness depends on both fiber radius and interphase modulus.

4.2. Effect of the Strength of Adhesion on the Curvature at the Edge of the Contact Zone

The interphase is described as a shell in contact with the hemisphere. We first recall the asymptotic models of the shell, as developed by Destuynder [22, 23]. A small parameter characteristic of curvature effects is defined as $\eta = \varepsilon \cdot \|\mathrm{Tr}((\partial N/\partial m)\cdot(\partial N/\partial m))^{1/2}\|$, where the norm of the maximum on the mean surface of the shell has been chosen. Different situations are obtained according to the relation between the thickness and parameter η, in terms of infinitesimally small quantities. One is particularly interested in two limit situations:

i) $\eta = \varepsilon$: this case is that of strongly curved shells; it is then found that the asymptotic development of the stress field starts with a term in ε^{-1}, except that for the normal stress the development starts in ε^{-2};
ii) $\eta = \varepsilon^2$: this corresponds to weakly curved shells. The asymptotic model obtained is then equivalent to the Novozhilov-Donnel model, and the solution starts with a term in ε^{-2}, *i.e.* (σ^{-2}, u^{-2}) is the unique solution of the system of equations describing the equilibrium of the shell. Considering a purely normal loading (such that applied tranctions are directed towards the normal to the shell) with normal stresses g_3^+ and g_3^- on the upper and lower surface of the shell, respectively, the unique solution is given explicitly as: the normal displacement is independent of the thickness coordinate, whereas the transverse shear and normal stresses are given by (see Destuynder [22, 23]:

$$\sigma_S = \frac{3}{4}(1 - z^2)\,\mathrm{div}(m_t) \tag{32}$$

$$\sigma_N = -g_3^- + \frac{(3z - z^3 + 2)}{2}\frac{(g_3^- + g_3^+)}{2} + \frac{z(z^2 - 1)}{4}$$

$$\mathrm{Tr}\left(n_t \frac{\partial N}{\partial m}\right) + \frac{3}{4}(z^2 - 1)\,\mathrm{Tr}\left(m_t \frac{\partial N}{\partial m}\right) \tag{33}$$

where n_t is the resulting effort (integration of the tangential displacement through the shell thickness) and m_t is the flexion momentum in the shell (integration of the tangential stress). We consider in the present situation that the change of curvature which occurs when the layer leaves the surface of the hemisphere is weak, so that the interphase obeys the weakly-curved shell model (consider a practical situation with $R = 2 \times 10^{-3}$ m, $t = 10^{-6}$ m, a cylindrical layer having a diameter $L = 10^{-3}$ m, so that $\varepsilon = 10^{-3}$; the ratio η/ε is equal to the inverse of the curvature radius 0.05, so that $\eta = 5 \times 10^{-6}$ is of the order of ε^2).

The rupture stress at the point of contact, $\sigma_R = \sqrt{2 \cdot Ku \cdot Ga}/\sqrt{t}$, is then identified with the normal stress in the middle plane of the shell ($z = 0$) at the point of contact, given by the asymptotic model, Equation (33) *i.e.*

$$\sigma_n = -\frac{2 \cdot E}{3R(1 - \nu)} t^4 \left(\frac{\partial u_n}{\partial \theta}\cot\theta + \frac{\partial^2 u_n}{\partial \theta^2}\right) \tag{34}$$

so that one deduces

$$\frac{\partial^2 u_z}{\partial \theta^2} = \frac{1}{2}\cos\theta_c(1 + \sqrt{1 + 4K}), \text{ with } K = \frac{2(1 - \nu)\sqrt{2K_u G_a}}{3Et^{9/2}}$$

The radius of curvature is then the product of two terms:

$$R_c = \frac{R}{\cos^2\theta_c} \cdot \frac{1}{1 + 2 \cdot (1 + \sqrt{(1 + K)})}, \tag{35}$$

The first term describes purely geometrical models (when adhesion energy is null, $K = 0$), while the second factor describes the effects of the strength of bonding between both surfaces.

Considering the value of the interphase thickness determined previously, $t = 0.75$ μm, and mechanical properties equal to those of the elastic film ($E = 1$ MPa, $\nu = 0.49$), the coefficient K is equal to 1.3×10^{26} and the curvature at the contact point becomes infinite, so that the elastic film leaves the surface of the hemisphere with a sudden large change of curvature, which is in fact observed during the measurements.

We lastly evaluate the curvature effect without the effect of adhesion forces; we assume, therefore, that the change of curvature at the edge of the contact zone is weak, and consider a thin slice of the layer, which we identify with a weakly curved shell. One part of it is in contact with the hemisphere (the "interior" zone), and is prolonged by a part outside the contact area (the "exterior" zone). The radius of curvature at the point of contact is then evaluated from the condition of the free surface, *i.e.* particularly the normal traction, Equation (34), is null, which implies:

$$\left(\frac{\partial u_n}{\partial \theta}\cot\theta + \frac{\partial^2 u_n}{\partial \theta^2}\right) = 0,$$

the radius of curvature being

$$R_c = \frac{\left(1 + \left(\frac{\partial u_z}{\partial x}\right)^2\right)^{3/2}}{\frac{\partial^2 u_z}{\partial x^2}},$$

with $x = R\sin\theta$ and $z = R\cos\theta$, so that

$$R_c = \frac{R^2}{\cos\theta_c \frac{\partial^2 u_z}{\partial \theta^2}}$$

For small compressions, this expression reduces to:

$$R_c = \frac{R}{\cos^2\theta_c}, \tag{36}$$

so it is seen that the curvature is nearly constant for small indentations of the layer. Further, one recovers the expression (35) when the adhesion energy is null.

Forces necessary to detach the hemisphere from the elastic layer have been measured on the same traction machine. Using logarithmic axes, a linear relation between the rupture force (multiplied by the layer thickness) and the penetration is obtained, with a relatively large scatter: the slope lies, in fact, in the interval 1.96–3.64. Thus, the force/penetration function takes the power law form:

$$F = \frac{C}{t} \cdot h^k, \tag{37}$$

where C and k are constants. The values of the exponent k obtained for the different thicknesses suggest that it is about 3 (compare with the value 1.5 obtained during compression).

We lastly consider energetic aspects and evaluate both the energy stored by the system during the compression stage, and the contribution of this energy that is released during unloading as a driving force for the crack propagation, while the remaining part represents the dissipated energy. These energies are evaluated from the experimental measurement of the force-displacement relation over a compression-unloading cycle corresponding to a displacement of 0.3 mm, for the layers of thickness (3.29 mm; 9.8 mm; 19.6 mm). The energy stored during compression is simply the integral

$$W^e = \int_0^{-0.3} F_c \, dh, \tag{38}$$

where F_c is the compression force. The energy balance during unloading is now:

$$\int_A \underline{t} \cdot \underline{\dot{u} \cdot dA} = \frac{dW^e}{dt} + P^R, \tag{39}$$

where P^R is the time derivative of the energy dissipated during failure. Viscoelastic losses have been assumed negligible compared with the

TABLE III Energies involved during a compression-unloading cycle (amplitude 0.3 mm)

layer thickness (mm)	3.29	9.8	19.6
Elastic energy stored (mJ)	1.36	0.67	0.589
Released energy (mJ)	1.227	0.541	0.377
Dissipated energy (mJ)	0.131	0.129	0.212

other energy contributions. One deduces then:

$$P^R = \int_A \underline{t}\cdot\dot{\underline{u}}\cdot dA - \int \underline{\underline{\sigma}}\cdot\dot{\underline{\underline{\varepsilon}}}\cdot dV = \int_A (\underline{t}\cdot\dot{\underline{u}}\cdot - u\cdot\dot{t})dA, \tag{40}$$

using the equilibrium equation and Green's formula. This last quantity is nothing else than the area delimited by the compression and unloading curves; evaluation of energy dissipated during failure then follows directly from the recording of the loading parameters (displacement and force). Energies involved during a cycle are listed in Table III below.

It is seen that the stored elastic energy increases when the thickness of the layer decreases, while the relative contribution of energy dissipated during rupture increases with the thickness.

5. CONCLUSION

A geometrically non-linear model of the contact between a rigid hemisphere and a thin elastic layer has been established, in which the contact law of the film is deduced from an asymptotic expansion method. The area of contact between the hemisphere and the film varies linearly with the depth of penetration of the hemisphere, considering penetrations much smaller than the layer thickness. The compressive effort exerted by the hemisphere is then determined as a quadratic function of the penetration, which is seen to describe correctly experimental measurements. It is though that such a method could be extended to the analysis of contact problems involving thin films in contact with punches of arbitrary profiles; consideration of the effect of the thickness involves either the determination of higher order terms in the asymptotic development of the solution, or a numerical treatment, as was done by the present author [24] in the case of a rigid, flat, cylindrical punch compressing an elastic layer. The effect of adhesion energy on the curvature effects at the edge of the contact zone has been assessed theoretically: when adhesion is weak, the elastic layer leaves the surface of the hemisphere in a smooth way, *i.e.* there is continuity of the curvature, whereas a sudden change of curvature occurs under strong adhesion conditions. Further, the comparison of the experimental rupture force with that evaluated from an asymptotic model provides an evaluation of the thickness of an hypothetical interphase between both solids, the measurement of which is a difficult task. A possible development of this study is the integration and modelling of adhesion forces, see Barquins [18], which are already important at the establishment of the contact.

References

[1] Goland, M. and Reissner, E., *J. Appl. Mech., ASME Trans.* **66**, A17–A27 (1944).
[2] Mitropoulos, C. and Sayir, M., *Z. Angew. Math. Phys.* **31**, 325–329 (1980).
[3] Klarbring, A., *Computer Methods in Applied Mechanics and Engineering* **96**, 329–350 (1992).
[4] Ciarlet, P. G. and Destuynder, Ph., *J. de mécanique* **18**, N°2, 315–344 (1979).
[5] Verhulst, F., *Asymptotic Analysis II* (Springer, Berlin, 1979).
[6] Lions, J. L., *Perturbations Singulières dans les Problèmes aux limites et en Contrôle Optimal*, Lecture Notes in Mathematics, **323** (Springer-Verlag, Berlin, 1973).
[7] Goldenveizer, A. L., *J. Appl. Math. Mech.* **26**, 1000–1025 (1964).
[8] Friedrichs, K. O. and Dressler, R. F., *Comm. Pure Appl. Math.* **14**, A7–A14, 1–33 (1961).
[9] Eckhaus, W., *Asymptotic Analysis of Singular Perturbations* (North-Holland, Amsterdam, 1979).
[10] Washizu, K., *Variational Methods in Elasticity and Plasticity*, 2nd ed. (Pergamon, Oxford, 1975).
[11] Valid, R., *Mechanics of Continuous Media and Analysis of Structures* (North-Holland, Amsterdam, 1981).
[12] Klarbring, A., *Int. J. Engng Sci.* **29**, N°4, 493–512 (1991).
[13] Reddy, J. N. and Roy, S., *Int. J. Non-Linear Mech.* **23**, 97–112 (1988).
[14] Klarbring, A., *Computer Methods in Applied Mechanics and Engineering* **96**, 329–350 (1992).
[15] Johnson, K. L., *Contact Mechanics* (Cambridge University Press, 1985).
[16] Matthewson, M. J., *J. Mech. Phys. Solids* **29**, N°2, 89–113 (1981).
[17] Maugis, D., *J. Adhesion Sci. Tech.* **1**, 105–134 (1987).
[18] Maugis, D. and Barquins, M., *J. Phys., Appl. Phys.* **11**, 1989–2023 (1978).
[19] Sneddon, I. N., *Int. J. Engng. Sci.* **3**, 45–57 (1965).
[20] Theocaris, P. S., "Models for adhesive joints between phases in sized composites". In Proceedings of the European Colloquium 227 (Saint-Etienne, France, 31/08–2/09). Verchery. G and Cardon, A. H., Eds., pp. 523–535 (1987).
[21] Destuynder, P., *Int. J. for Num. Methods in Engng.* **35**, 1237 (1982).
[22] Destuynder, P., *Acta Applicandae.*, Mathematical N°4, 15 (1985).
[23] Destuynder, P., *Modélisation des coques minces élastiques* (MASSON, Paris, 1990).
[24] Ganghoffer, J. F. and Gent, A. N., *J. Adhesion* **48**, 75–84 (1995).

APPENDIX 1

Asymptotic Modelling of Geometrically Nonlinear Thin Plates

The problem is stated in the form of a Hellinger-Reissner variational principle:

$$\text{Find } (S, \phi) \in \Sigma^\varepsilon \times V^\varepsilon \text{ such that}$$

$$(P) \qquad A^\varepsilon(S, \tau) + B^\varepsilon(\tau, \phi) = 0, \quad \forall\, \tau \in \Sigma^\varepsilon$$

$$B^\varepsilon(S, \psi) = F^\varepsilon(\psi), \quad \forall\, \psi \in V^\varepsilon$$

where Σ^ε is the set of symmetrical tensors, while V^ε is the set of kinematically admissible placement fields, *i.e.* fields such that the displacement field satisfies previous boundary conditions. The forms A^ε, B^ε and the linear form F^ε are defined by:

$$A^\varepsilon(S, \tau) = \int_{\Omega_1^\varepsilon \cup \Omega_2^\varepsilon} a_{ijkl} S_{ij} \tau_{kl}\, dx^\varepsilon + \int_{\Omega_0^\varepsilon} \left(\frac{1+\nu}{E} S_{ij} - \frac{\nu}{E} \delta_{ij} S_{kk} \right) \tau_{ij}\, dx^\varepsilon$$

$$B^\varepsilon(\tau, \phi) = -\int_{\Omega^\varepsilon} \tau_{ij} E_{ij}(\phi)\, dx^\varepsilon; \quad F^\varepsilon(\phi) = -\int_{\Omega^\varepsilon} f_i \phi_i \cdot dx^\varepsilon - \int_{S^\varepsilon} t_i \phi_i \cdot ds^\varepsilon$$

Note that the functional spaces Σ^ε, V^ε must be chosen in such a way that the product $\tau_{ij} E_{ij}(\phi)$ is integrable in B^ε. These variational equations can be shown to be equivalent to the differential equations governing equilibrium of the three-body system, including the conditions of continuity of the displacement and traction vectors at both contact surfaces.

As a first step towards obtaining an approximate solution of the original problem, we consider a unidirectional zoom in the thickness direction, which defines an equivalent problem but posed now over a non-dimensional domain (Fig. A1).

The geometrical change of the domain is defined mathematically through the following coordinates changes: to each point, y, of the transformed domain, Ω, we associate a point, x, of the initial domain,

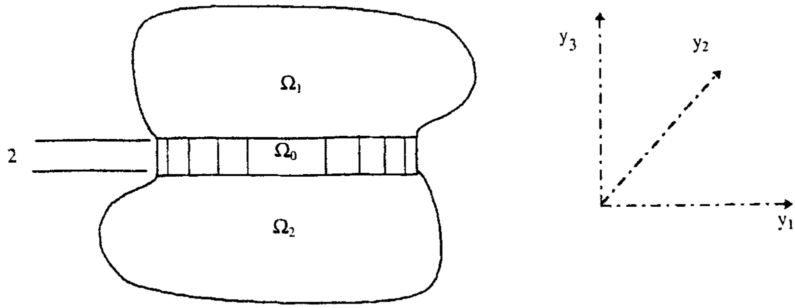

FIGURE A1 A dimensional domain.

Ω^ε, through the correspondences:

$$y = (y_1, y_2, y_3) \in \Omega_0 \to x = (y_1, y_2, \varepsilon \cdot y_3) \in \Omega_0^\varepsilon$$

$$y = (y_1, y_2, y_3) \in \Omega_1 \to x = (y_1, y_2, y_3 - 1 + \varepsilon) \in \Omega_1^\varepsilon$$

$$y = (y_1, y_2, y_3) \in \Omega_2 \to x = (y_1, y_2, y_3 + 1 - \varepsilon) \in \Omega_2^\varepsilon$$

The transformation of the geometry induces a transformation of the displacement and stress fields, according to:

$$\phi(x) = \phi^\varepsilon(y)\,; \;\; v(x) = v^\varepsilon(y); \;\; \tau(x) = \tau^\varepsilon(y)$$

$$A_{ijkl}(x) = \bar{A}_{ijkl}(y).$$

Applied forces and elasticity coefficients transform according to:

$$f(x) = \bar{f}(y); \;\; t(x) = \bar{t}(y);$$

$$A_{ijkl}(x) = \bar{A}_{ijkl}(y); \;\; a_{ijkl}(x) = \bar{a}_{ijkl}(y); \;\; v(x) = \bar{v}(y); \;\; E(x) = \bar{E}(y)$$

We first consider the effect of the change of the geometry on the different components of the strain tensor. We notice that the definition of the placement (Equation (1)) implies following change:

$$\bar{\phi}_\alpha = \phi_\alpha\,; \;\; \phi_3 = \varepsilon \cdot \bar{\phi}_3$$

According to this, the strain components transform as:

$$\bar{E}_{\alpha\beta} = E_{\alpha\beta};$$

$$E_{\alpha 3} = \frac{1}{2\varepsilon}\cdot\left(\frac{\partial\bar{\phi}_1}{\partial Y_\alpha}\cdot\frac{\partial\bar{\phi}_1}{\partial Y_3} + \frac{\partial\bar{\phi}_2}{\partial Y_\alpha}\cdot\frac{\partial\bar{\phi}_2}{\partial Y_3} + \frac{\partial\bar{\phi}_1}{\partial Y_\alpha}\cdot\frac{\partial\bar{\phi}_2}{\partial Y_3} + \frac{\partial\bar{\phi}_2}{\partial Y_\alpha}\cdot\frac{\partial\bar{\phi}_1}{\partial Y_3}\right)$$

$$+\frac{1}{2}\cdot\left(\frac{\partial\bar{\phi}_3}{\partial Y_\alpha}\cdot\frac{\partial\bar{\phi}_3}{\partial Y_3} + \frac{\partial\bar{\phi}_1}{\partial Y_\alpha}\cdot\frac{\partial\bar{\phi}_3}{\partial Y_3} + \frac{\partial\bar{\phi}_2}{\partial Y_\alpha}\cdot\frac{\partial\bar{\phi}_3}{\partial Y_3} + \frac{\partial\bar{\phi}_3}{\partial Y_\alpha}\cdot\frac{\partial\bar{\phi}_1}{\partial Y_3} + \frac{\partial\bar{\phi}_3}{\partial Y_\alpha}\cdot\frac{\partial\bar{\phi}_2}{\partial Y_3}\right); \tag{A1}$$

$$E_{33} = \frac{1}{2\cdot\varepsilon^2}\cdot\left(\frac{\partial\bar{\phi}_1}{\partial Y_3}\cdot\frac{\partial\bar{\phi}_1}{\partial Y_3} + \frac{\partial\bar{\phi}_2}{\partial Y_3}\cdot\frac{\partial\bar{\phi}_2}{\partial Y_3} + 2.\frac{\partial\bar{\phi}_1}{\partial Y_3}\cdot\frac{\partial\bar{\phi}_2}{\partial Y_3}\right)$$

$$+\frac{1}{\varepsilon}\cdot\left(\frac{\partial\bar{\phi}_3}{\partial Y_3}\cdot\frac{\partial\bar{\phi}_1}{\partial Y_3} + \frac{\partial\bar{\phi}_3}{\partial Y_3}\cdot\frac{\partial\bar{\phi}_2}{\partial Y_3}\right) + \frac{1}{2}\cdot\left(\frac{\partial\bar{\phi}_3}{\partial Y_3}\cdot\frac{\partial\bar{\phi}_3}{\partial Y_3} - 1\right) \tag{A2}$$

so that it is seen that the strain components $E_{\alpha 3}$ and E_{33} contain each contribution which scales differently according to the power of the small parameter involved:

$$E_{\alpha 3} = \varepsilon^{-1}\cdot\bar{E}_{\alpha 3}^{-1} + \bar{E}_{\alpha 3}^{0};\ E_{33} = \varepsilon^{-2}\cdot\bar{E}_{33}^{-2} + \varepsilon^{-1}\cdot\bar{E}_{33}^{-1} + \bar{E}_{33}^{0},$$

where the components $\bar{E}_{\alpha 3}^{-1}$, $\bar{E}_{\alpha 3}^{0}$, $\bar{E}_{33}^{-2}$, $\bar{E}_{33}^{-1}$, $\bar{E}_{33}^{0}$ are identified from Equations (A1) and (A2).

As a consequence, no simple relation between the original and the tranformed strain can be found. The stress components are assumed to transform according to:

$$\bar{S}_{\alpha 3} = \varepsilon^{-1}S_{\alpha 3};\ \bar{S}_{33} = \varepsilon^{-2}\bar{S}_{33};\ \bar{S}_{\alpha\beta} = S_{\alpha\beta}.$$

ε is the perturbation parameter, the choice of which is dictated from considerations about both relative geometrical and mechanical parameters characteristic of the bodies. Since we assume that the adhesive is much softer than the two adherends, it is natural to assume that the modulus of the adhesive scales as:

$$\bar{E} = \varepsilon\cdot E_0 \tag{A3}$$

where E_0 has the order of magnitude of the modulus of the adherends. Considering $(S^\varepsilon, \phi^\varepsilon)$ the transformed solution, problem (P) expresses now over the new domain as:

$$\text{Find } (S^\varepsilon, \phi^\varepsilon) \in \Sigma \times V \text{ such that}$$

$$(P^\varepsilon) \quad A^0(S^\varepsilon, \tau) + \varepsilon^2 \cdot A^2(S^\varepsilon, \tau) + \varepsilon^4 \cdot A^4(S^\varepsilon, \tau) + B(\tau, \phi^\varepsilon) = 0, \quad \forall\, \tau \in \Sigma$$

$$B(S^\varepsilon, \psi) = \varepsilon^{-1} \cdot F^{-1}(\psi) + F^0(\psi) + \varepsilon \cdot F^1(\psi), \quad \forall\, \psi \in V$$

where

$$A^0(S, \tau) = \int_{\Omega_0} \frac{1}{E_0}((1+\bar{\nu}) \cdot S_{\alpha\beta} - \bar{\nu} \cdot \delta_{\alpha\beta} \cdot S_{\alpha\alpha})\tau_{\alpha\beta} \cdot dx + \int_{\Omega_1 \cup \Omega_2} a_{ijkl} S_{ij} \tau_{kl} \cdot dx;$$

$$A^2(S, \tau) = \int_{\Omega_0} \left(2\frac{(1+\bar{\nu}) \cdot}{E_0} S_{\alpha 3} \cdot \tau_{\alpha 3} - \frac{\bar{\nu} \cdot}{E_0}(S_{33} \cdot \tau_{\mu\mu} + S_{\mu\mu} \cdot \tau_{33}) \right) \cdot dx;$$

$$A^4(S, \tau) = \int_{\Omega_0} \frac{1}{E_0} S_{33} \cdot \tau_{33} \cdot dx;$$

$$B^1(\tau, \psi) = -\int_{\Omega_0} \tau_{\alpha\beta} \bar{E}_{\alpha\beta}(\psi) \cdot dx - \int_{\Omega_0} \tau_{\alpha\beta} \bar{E}_{\alpha 3}^{-1}(\psi) \cdot dx - \int_{\Omega_0} \tau_{33} \bar{E}_{33}^{-2}(\psi) \cdot dx;$$

$$B^0(\tau, \psi) = -\int_{\Omega_1 \cup \Omega_2} \tau_{ij} \bar{E}_{ij}(\psi) \cdot dx;$$

$$B^2(\tau, \psi) = -\int_{\Omega_0} \tau_{\alpha 3} \bar{E}_{\alpha 3}^0(\psi) \cdot dx - \int_{\Omega_0} \tau_{33} \bar{E}_{33}^{-1}(\psi) \cdot dx;$$

$$B = B^0 + \varepsilon \cdot B^1 + \varepsilon^2 \cdot B^2;$$

$$F^0(\psi) = -\int_{\Omega_0} \bar{f}_3 \psi_3 \cdot dx - \int_{S_1 \cup S_2} \bar{t}_\alpha \psi_\alpha \cdot dx - \int_{S_1 \cup S_2} \bar{f}_i \psi_i \cdot dx;$$

$$F^{-1}(\psi) = -\int_{S_1 \cup S_2} \bar{t}_3 \psi_3 \cdot dx$$

$$F^1(\psi) = -\int_{\Omega_0} \bar{f}_\alpha \psi_\alpha \cdot dx$$

Problem (P^{ε}) is then expressed in terms of the displacement, which involves a split of the strain tensor into a linear and a non-linear part, according to:

$$E_{ij}(v)=\frac{1}{2}\left(\frac{\partial v_i}{\partial X_j}+\frac{\partial v_j}{\partial X_i}\right)+\frac{1}{2}\frac{\partial v_k}{\partial X_j}\frac{\partial v_k}{\partial X_i}=L(E_{ij}(v))+NL(E_{ij}(v))$$

We now assume that the solution of problem (P^{ε}) can be expressed as the asymptotic developments

$$S^{\varepsilon}=\varepsilon^{-2}S^{-2}+\varepsilon^{-1}S^{-1}+S^{0}+\cdots$$

$$u^{\varepsilon}=\varepsilon^{-2}u^{-2}+\varepsilon^{-1}u^{-1}+u^{0}+\cdots$$

where the successive coefficients of the powers of ε are independent of ε. The need to start the development with a term in ε^{-2} comes from the scaling of the strain component E_{33}^{-2} under the coordinate transformation (Equation (A2)). Inserting these development into problem (P^{ε}) results in variational equations that must be satisfied whatever the ε, and consequently, the successive powers must be zero. Therefore, the coefficient of term ε^{-2} must be zero, so that:

(P^{-3})
$$B^{1}(\tau,NL(E(u^{-2})))=0,\quad \forall\,\tau\in\Sigma;$$

(P^{-2})
$$A^{0}(S^{-2},\tau)+B^{0}(\tau,L(E(u^{-2})))+B^{0}(\tau,NL(E(u^{-1})))$$
$$+B^{2}(\tau,NL(E(u^{-2})))=0,\quad \forall\,\tau\in\Sigma$$

(P^{-1})
$$A^{0}(S^{-1},\tau)+B^{0}(\tau,L(E(u^{-1})))+B^{1}(\tau,NL(E(u^{-1})))$$
$$+B^{1}(\tau,L(E(u^{-2})))=0,\quad \forall\,\tau\in\Sigma$$
$$B^{1}(S^{-2},v)=F^{-1}(v),\quad \forall\,v\in V$$

(P^{0})
$$A^{0}(S^{0},\tau)+A^{2}(S^{-2},\tau)+B^{0}(\tau,L(E(u^{-0})))+B^{1}(\tau,L(E(u^{-1})))$$
$$+B^{2}(\tau,NL(E(u^{-1})))+B^{2}(\tau,L(E(u^{-2})))=0,\quad \forall\,\tau\in\Sigma$$
$$B^{1}(S^{-1},v)+B^{2}(S^{-2},v)=F^{0}(v),\quad \forall\,v\in V$$

The second equality in (P^{-1}) implies in the adhesive part that

$$\int_{\Omega_0} S_{\alpha 3}^{-2}\bar{E}_{\alpha 3}^{-2}(v)dx + \int_{\Omega_0} S_{\alpha\beta}^{-2}\bar{E}_{\alpha\beta}(v)dx + \int_{\Omega_0} S_{\alpha 3}^{-2}\bar{E}_{\alpha 3}^{-1}(v)dx$$

$$+ \int_{\Omega_0} S_{33}^{-2}\bar{E}_{33}^{-2}(v)dx = 0, \quad \forall\, v \in V$$

and one duduces (using Green's equality) that

$$S_{i3,3}^{-2} = 0 \tag{A4}$$

The traction vector is then constant through the adhesive thickness.

The first equality in (P^{-2}) is explicitly (in the adhesive part):

$$\int_{\Omega_0} \frac{1}{E_0}((1+\bar{\nu})\cdot S_{\alpha\beta}^{-2} - \bar{\nu}\cdot\delta_{\alpha\beta}\cdot S_{\alpha\alpha}^{-2})\tau_{\alpha\beta}\cdot dx$$

$$= \int_{\Omega_0} \tau_{33} NL(\bar{E}_{33}^{-1}(u^{-2}))dx + \int_{\Omega_0} \tau_{\alpha 3} NL(\bar{E}_{\alpha 3}^{0}(u^{-2}))dx, \quad \forall\, \tau \in \Sigma.$$

This implies that the in-plane stress field is given by

$$S_{12}^{-2} = 0$$

$$S_{11}^{-2} - \nu\cdot S_{22}^{-2} = 0$$

$$-\nu\cdot S_{11}^{-2} + S_{22}^{-2} = 0$$

and therefore the in-plane stress tensor is null:

$$S_{12}^{-2} = 0; \quad S_{11}^{-2} = S_{22}^{-2} = 0, \tag{A5}$$

so that the stress tensor is constant through the adhesive thickness.

The behaviour law of the adhesive, Equation (3), implies then following expression for the in-plane strain components

$$E_{12} = 0; \quad E_{11} = E_{22} = -\frac{\nu}{E} S_{33} \tag{A6}$$

whereas Klarbring (1992) assumes it is zero. The constitutive law, Equation (3), together with Equations (A4) and (A5) implies now

$$\bar{E}_{33}^{-2} = \frac{1}{E} \cdot \bar{S}_{33}^{-2}, \text{ so that}$$

$$\bar{E}_{33,3}^{-2} = 0 \tag{A7}$$

which from the definition, Equation (1), of $\bar{E}$ implies that $\partial^2 \phi / \partial X_3^2 = 0$, and therefore the placement varies linearly through the adhesive thickness:

$$\phi(X) = \frac{1}{2} \cdot (\phi^1(X) + \phi^2(X)) + \frac{X_3}{h} \cdot (\phi^1(X) - \phi^2(X)), \tag{A8}$$

where ϕ^1, ϕ^2 are the traces of ϕ on S_1^ε, S_2^ε respectively.

It can then be concluded that the adhesive can be treated as a material surface, *i.e.* the mechanical field solution of the "first order" problem does not involve the thickness coordinate, but can be expressed only *via* their traces on the two interfaces.

We further derive a series of equalities from problems (P^ε) (first equalities) in order to characterise the strain tensor in the adhesive part:

$$NL(\bar{E}_{33}^{-2,-2}) = 0 \tag{A9a}$$

$$NL(\bar{E}_{\alpha 3}^{-1,-2}) = 0 \tag{A9b}$$

$$NL(\bar{E}_{\alpha\beta}^{\cdot,-2}) = 0 \tag{A9c}$$

$$NL(\bar{E}_{\alpha 3}^{0,-2}) = 0 \tag{A9d}$$

$$NL(\bar{E}_{33}^{-1,-2}) = 0 \tag{A9e}$$

$$L(\bar{E}_{\alpha\beta}^{\cdot,-1}) = \frac{1+\bar{\nu}}{E_0} S_{\alpha\beta}^0 - \frac{\bar{\nu}}{E_0} \delta_{\alpha\beta} S_{\alpha\alpha}^0 \tag{A9f}$$

$$NL(\bar{E}_{\alpha 3}^{-1,-1}) + L(\bar{E}_{\alpha 3}^{-1,-2}) = 0 \tag{A10a}$$

$$NL(\bar{E}_{\alpha\beta}^{\cdot,-1}) + L(\bar{E}_{\alpha\beta}^{\cdot,-2}) = 0 \tag{A10b}$$

$$NL(\bar{E}_{33}^{-2,-1}) + L(\bar{E}_{33}^{-2,-2}) = 0 \tag{A10c}$$

$$L(\bar{E}_{33}^{-2,-1}) + NL(\bar{E}_{33}^{-1,-1}) + L(\bar{E}_{33}^{-1,-2}) = 0 \tag{A10d}$$

$$L(\bar{E}_{\alpha 3}^{-1,-1}) + NL(\bar{E}_{\alpha 3}^{0,-1}) + L(\bar{E}_{\alpha 3}^{0,-2}) = 2 \cdot \frac{1+\bar{\nu}}{E_0} S_{\alpha 3}^{-2} \tag{A10e}$$

In a term such as $\bar{E}^{-i,-j}$, the superscript i stands for the strain component defined in Equations (A1), (A2) and the second j denotes the order of the corresponding term in the asymptotic expansion.

From (P^0), we deduce (considering a virtual field τ null in Ω_0) that $A^0(S^0, \tau) = 0$, $\forall\, \tau$, which implies $S^0 = 0$, and therefore from (A9f):

$$NL(\bar{E}_{\alpha\beta}^{-2}) = 0 \tag{A11a}$$

$$L(\bar{E}_{\alpha\beta}^{\cdot,-1}) = 0 \tag{A11b}$$

so that the non-linear part of the strain tensor in the adhesive plane is zero. Further, Equations (A9a, b, c, e) imply that the components $\bar{E}^{-2}$ and $\bar{E}_{\alpha\beta}$ of the strain tensor can be represented by their associated linearized strain measures (at the principal order).

The two systems formed, respectively, by Equations (A9a, b, c, d, e) and (A10a, c, d, e) decouple, so no further information concerning the strain tensor can be gained.